doi:10.1016/j.jmb.2011.02.004 J. Mol. Biol. (2011) 408, 74–86

Contents lists available at www.sciencedirect.com

Journal of Molecular Biology

journal homepage: http://ees.elsevier.com.jmb

Crystal Structures of *Xanthomonas* Small Heat Shock Protein Provide a Structural Basis for an Active Molecular Chaperone Oligomer

Eduardo Hilario[1], Francisco Javier Medrano Martin[2], Maria Célia Bertolini[3] and Li Fan[1]*

[1]*Department of Biochemistry, University of California, Riverside, 2482B Boyce Hall, Riverside, CA 92521-0123, USA*
[2]*Centro de Biologia Molecular e Estrutural, LNLS, Campinas, SP, Brazil 13083-970*
[3]*Departamento de Bioquimica e Tecnologia Quimica, Instituto de Quimica, UNESP, Araraquara, SP, Brazil 14800-900*

Received 12 October 2010; received in revised form 27 January 2011; accepted 2 February 2011
Available online 15 February 2011

Edited by R. Huber

Keywords:
α-crystallin domain;
protein folding;
cataracts;
citrus canker;
heat shock response

Small heat shock proteins (sHsps) are ubiquitous low-molecular-weight chaperones that prevent protein aggregation under cellular stresses. sHsps contain a structurally conserved α-crystallin domain (ACD) of about 100 amino acid residues flanked by varied N- and C-terminal extensions and usually exist as oligomers. Oligomerization is important for the biological functions of most sHsps. However, the active oligomeric states of sHsps are not defined yet. We present here crystal structures (up to 1.65 Å resolution) of the sHspA from the plant pathogen *Xanthomonas* (XaHspA). XaHspA forms closed or open trimers of dimers (hexamers) in crystals but exists predominantly as 36mers in solution as estimated by size-exclusion chromatography. The XaHspA monomer structures mainly consist of α-crystallin domain with disordered N- and C-terminal extensions, indicating that the extensions are flexible and not essential for the formation of dimers and 36mers. Under reducing conditions where α-lactalbumin (LA) unfolds and aggregates, XaHspA 36mers formed complexes with one LA per XaHspA dimer. Based on XaHspA dimer–dimer interactions observed in crystals, we propose that XaHspA 36mers have four possible conformations, but only XaHspA 36merB, which is formed by open hexamers in 12mer-6mer-6mer-12mer with protruding dimers accessible for substrate (unfolding protein) binding, can bind to 18 reduced LA molecules. Together, our results unravel the structural basis of an active sHsp oligomer.

Introduction

Small heat shock proteins (sHsps) are a diverse group of molecular chaperones whose molecular masses range from 12 to 43 kDa. The importance of sHsps is evidenced by their presence in all kingdoms of life and the implication that sHsps are related to a range of diseases including cataracts,[1] myopathy,[2] aging and aging-related disease,[3] neuropathy, and tumor growth and development. [4–6] Although new physiological roles for sHsps are emerging, the majority of sHsps primarily function as ATP-indepen-

*Corresponding author. E-mail address: lifan@ucr.edu.

Abbreviations used: ACD, α-crystallin domain; LA, α-lactalbumin; LAred, reduced LA; MjHsp16.5, *Methanococcus jannaschii* Hsp16.5; WHsp16.9, wheat Hsp16.9; sHsp, small heat shock protein; Xac, *Xanthomonas axonopodis* pv. *citri*; XaHspA, sHsp A from *Xanthomonas axonopodis* pv. *citri*; PDB, Protein Data Bank; MR, molecular replacement; RT, room temperature.

dent chaperones by binding proteins in nonnative conformation under cellular stresses to avoid irreversible aggregation of unfolding proteins.[7–10]

sHsps share a conserved domain of ~100 amino acid residues characterized by the α-crystallin domain (ACD) flanked by varied N- and C-terminal extensions that contribute to the sequence and structural diversity among sHsps. sHsps usually form large oligomers with a molecular mass of up to 1000 kDa and show great variations in size and subunit organization as well. The importance of both extensions for sHsps oligomerization, quaternary dynamics, and chaperone activity has been described in a variety of reviews.[8,11–13]

Structural studies of sHsps are limited even though sHsps have been identified from over 100 genomic sequences. Only six sHsps crystal structures were solved to date, including the parasitic flatworm Tsp36 protein [Protein Data Bank (PDB) code 2BOL],[14] wheat Hsp16.9 (WHsp16.9) (PDB code 1GME),[15] *Methanococcus jannaschii* Hsp16.5 (MjHsp16.5) (PDB code 1SHS),[16] rat Hsp20 (PDB code 2WJ5),[17] a truncated bovine αA-crystallin (PDB codes 3L1E and 3L1F),[18] and human αB-crystallin (PDB codes 2WJ7,[17] 2KLR,[19] and 3L1G[18]). These high-resolution structures have shown that the basic building block of sHsps is a dimer. Protein dimerization stabilizes the monomeric structure and allows the dimers to form different large multimeric structures. The oligomeric structure of MjHsp16.5 is composed of 24 monomers arranged in a globular shell-like structure,[16] while the WHsp16.9 oligomer is a dodecameric double disk arranged in a trimer of dimers.[15] Tsp36 contains two ACDs per monomer, but no oligomeric complex was described for Tsp36 except dimers and tetramers.[14]

Critical questions such as how sHsps bind protein substrates and act as molecular chaperones remain unclear. A number of different sHsps are shown to form large and stable complexes with nonnative proteins, preventing them from forming aggregates.[11–13,20] The current view is that sHsps can effectively interact with aggregation-prone folding intermediates under cellular stresses and maintain them in a conformation suitable for refolding mediated by ATP-dependent chaperones. A variety of experimental approaches using different sHsps and different protein substrates have been reported to identify potential binding sites on these molecular chaperones. Some evidence indicated that sHsp oligomerization prevents the binding motifs from being accessible; thus, they need to dissociate into smaller or dimeric sHsps for activation.[21] However, other studies show that sHsp oligomers can directly interact with nonnative proteins,[22] perhaps after conformational changes to shift sHsp oligomers to a binding mode.

In this work, we report three crystal structures of sHspA from the phytopathogenic bacterium *Xanthomonas citri* pv. *citri* (XaHspA), previously known as *Xanthomonas axonopodis* pv. *citri* (*Xac*), and investigated its interactions with α-lactalbumin (LA) and insulin in nonnative conformation. *Xac* causes citrus canker, one of the most serious diseases in many tropical and subtropical citrus crops and results in heavy economic losses to worldwide citrus plantations. Since the whole genome of this bacterium was sequenced several years ago,[23] functional genomic studies[24] and structural determination (PDB codes 2F1E, 2G3W, 2PXG, 3CNR, 3E4R, 3GLA, and 3GZG) have recently started to investigate Xac protein function and structure in order to uncover the pathogenic mechanisms of Xac-citrus infection. This report is the result of such effort, and our results shed light on the mechanism governing the formation of defined sHsp complexes with nonnative substrate proteins and the structural organization of these complexes.

Results

XaHspA ACD structure of XaHspA

The *HspA* gene from *Xac* encodes an sHsp (XaHspA) containing 158 amino acid residues (molecular mass of 17.9 kDa). XaHspA shares high sequence identity with sHsps from different *Xanthomonas* species but has low sequence identity with WHsp16.9 (23%), MjHsp16.5 (21%), and human αB-crystallin (17%). Despite the low sequence conservation of sHsps, our results show that XaHspA contains an ACD structure very similar to the ACD structures observed in WHsp16.9 and other sHsps (Fig. 1).

When the full-length XaHspA protein (plus a His-tag fused at the N-terminus) was used for crystallization, three crystal forms were obtained and diffracted up to 1.65 Å resolution with a synchrotron radiation light source. All crystals belong to the space group *H*3 or *R*3. The structure of the first crystal (PDB code 3GLA) was solved by the molecular replacement (MR) method using the WHsp16.9 dimeric structure (PDB code 1GME)[15] without the N- and C-terminal extensions. This refined structure was then used to solve the other two structures (PDB codes 3GT6 and 3GUF; for detailed statistics, see Table 1). There are two XaHspA monomers in the asymmetric unit cells to form a dimer in all crystals. The three refined XaHspA structures are almost identical (Fig. 1d) and are limited to the ACD structure. The first 36–40 residues at the N-terminal extension of XaHspA (plus the 36 residues tagged during cloning) and the last 19–22 C-terminal residues are not defined (Fig. 1a) due to lack of reliable densities in electron density maps. Analysis of crystal drops by SDS-

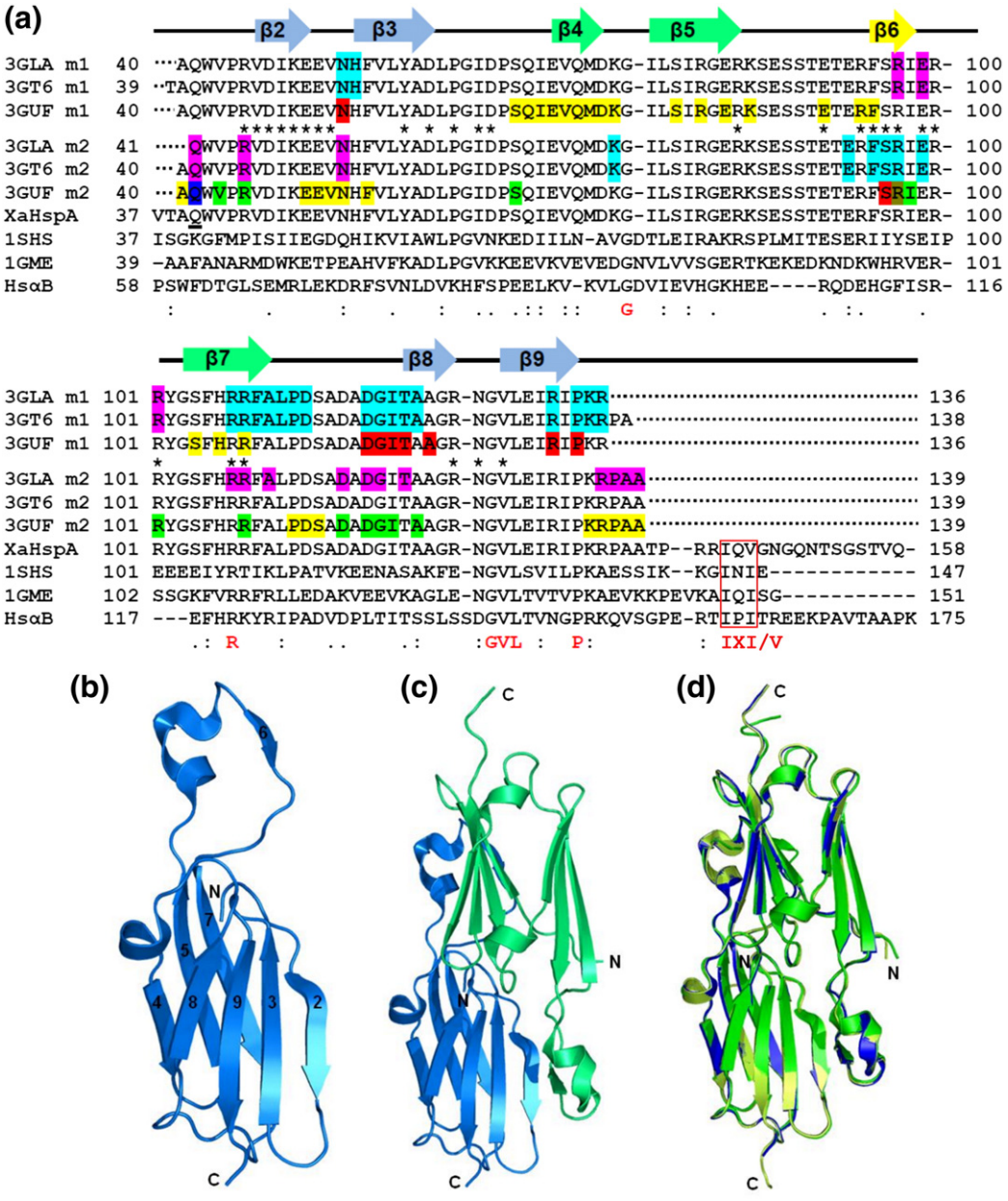

Fig. 1. Structure of the XaHspA protein and sequence comparisons with other sHsps. (a) Sequence alignment of XaHspA with MjHsp16.5 (1SHS), WHsp16.9 (1GME), and human αB-crystallin (HsαB) in the region of the ACD and C-terminal extension. Sequence alignment was analyzed by ClustalW2,[25] with sequence conservations indicated below the sequences by (.) for similar residues, (:) for highly similar residues, and a single letter for identical residues. The conserved IXI/V motif at the C-terminal extension is framed in a red box and indicated below the sequences. The two monomers of the XaHspA dimer in crystals (3GLA, 3GT6, and 3GUF) are indicated by m1 and m2. Dots within the sequences (3GLA, 3GT6, and 3GUF) represent the missing residues in the XaHspA crystal structures. Key residues contributing to subunit interactions within each dimer are indicated by (*) in the space between m1 and m2. Key residues involved in dimer–dimer interactions are highlighted in cyan and pink for crystals 3GLA and 3GT6 and yellow, green, and red for crystal 3GUF, respectively. β-Strands of XaHspA ACD are indicated by the labeled arrows above the sequences. β-Strands 2, 3, 8, and 9 (light-blue arrows) form one sheet, and β-strands 4, 5, and 7 (light-green arrows) form the other sheet to build a two-β-sheet sandwich. (b) Ribbon diagram of XaHspA monomeric structure in the crystal form I (3GLA) solved at 1.65 Å resolution. β-Sheets are numbered according to the convention used for WHsp16.9 and MjHsp16.5. (c) Ribbon diagram of the dimeric structure of the XaHspA 3GLA model. (d) Superposition of the dimers belonging to the crystal form I (3GLA model, blue), crystal form II (3GUF model, green), and crystal form III (3GT6 model, yellow). The structure figures were prepared with PyMOL.[26]

Table 1. Data collection and refinement statistics (MR)

	3GLA	3GUF	3GT6
Data collection			
Space group	*H*3 (no. 146)	*H*3 (no. 146)	*H*3 (no. 146)
Cell dimensions			
a, *b*, *c* (Å)	128.67, 128.67, 55.25	110.58, 110.58, 55.19	128.59, 128.59, 55.29
α, β, γ (°)	90.00, 90.00, 120.00	90.00, 90.00, 120.00	90.00, 90.00, 120.00
Resolution range (Å)	26.97-1.64 (1.73-1.64)	47.82-2.26 (2.38-2.26)	26.96-2.15 (2.26-2.15)
R_{merge}	4.7 (51.3)	3.4 (26.8)	4.9 (22.5)
I/sI	14.6 (2.4)	16.5 (3.1)	17.8 (5.5)
Completeness (%)	100.0 (100.0)	96.3 (76.2)	100.0 (100.0)
Redundancy	5.5 (5.2)	2.8 (2.6)	3.8 (3.7)
Refinement			
Resolution range (Å)	26.97-1.65	31.921-2.28	26.96-2.15
No. of reflections	38,974	10,862	17,719
R_{work}/R_{free}	0.202/0.236	0.239/0.289	0.199/0.237
No. of atoms			
Protein	1576	1575	1600
Phosphate	2	—	—
Water	247	35	148
B-factors			
Protein	25.42	42.99	25.46
Ligand/ion	36.83	—	—
Water	38.13	44.17	35.41
RMSD			
Bond lengths (Å)	0.034	0.022	0.024
Bond angles (°)	3.151	2.090	2.169

Values in parentheses are for the highest-resolution shell.

PAGE indicated that the majority of His-tagged XaHspA was still intact during crystallization (Fig. S1), suggesting that both terminal extensions are highly flexible. In addition, the two XaHspA monomers in all the crystal forms are different in length, with one having three more residues at the C-terminus (m2 in Fig. 1a). All together, these indicate that both termini exist in the crystal in spite of not being shown in the models. The ACD structure contains eight β-strands forming two antiparallel β-sheets. Like the ACD structure of WHsp16.9 15, β-strands 2, 3, 9, and 8 form one sheet, and β-strands 4, 5, and 7 form the other sheet, while β1 is absent (Fig. 1b). Strand β6 locates separately in a loop and forms part of the dimeric interface by pairing with strand β2 from another monomer to extend the β-sheet (Fig. 1c). Charges or polar interactions between charged side chains or main chains of neutral residues play a key role in XaHspA monomer–monomer interaction to form the dimer. The key residues (as indicated by stars in Fig. 1a) involved in dimerization are R45, V46 (main chain), D47, K49, E50, E51, Y58, D60, P62, I64 (main chain), D65, R84, E91, R94, F95, R97, E99, R100, R101, R107, N126, and V128.

Interactions between XaHspA dimers

In all crystals, XaHspA molecules form hexamers in the form of trimers of ACD dimers by crystal symmetry (Fig. 2a). Interestingly, crystals 3GUF and 3GT6 were obtained under the same condition, but the hexamers in 3GUF model are closed triangles (top, Fig. 2a), while the hexamers in model 3GT6 are opened triangles (bottom, Fig. 2a). The trimers of ACD dimers in crystal 3GLA are also open triangles even if they were crystallized under different conditions (Table 1). For all XaHspA crystal structures, each XaHspA hexamer interacts with six ACD dimers from three hexamers (red; the third ACD dimer of each hexamer is not shown, Fig. 2b) above and three ACD dimers from three hexamers (green; one ACD dimer per hexamer is shown, Fig. 2c) underneath. The interactions between XaHspA ACD dimers from different layers are dominated by polar or charge interactions (Fig. 1a and 2d). Each XaHspA ACD dimer has two surfaces with distinguished electrostatic potential features (Fig. 2d): the top surface has a zone of positive electrostatic potentials (blue in Fig. 2d) across the ACD dimer from T1 to T2, while the bottom surface has two separate patches, B1 and B2, with negative electrostatic potentials (red in Fig. 2d). Therefore, XaHspA ACD dimers from different layers of XaHspA hexamers cannot interact with each other through the same surface (neither top to top nor bottom to bottom). They have to interact with each other through the different surfaces (top to bottom) by two major interaction interfaces (B1 toT1 and B2 to T2, yellow circles). In all crystals, one ACD dimer uses the two interaction sites (T1 and T2) on the same surface to interact separately with different

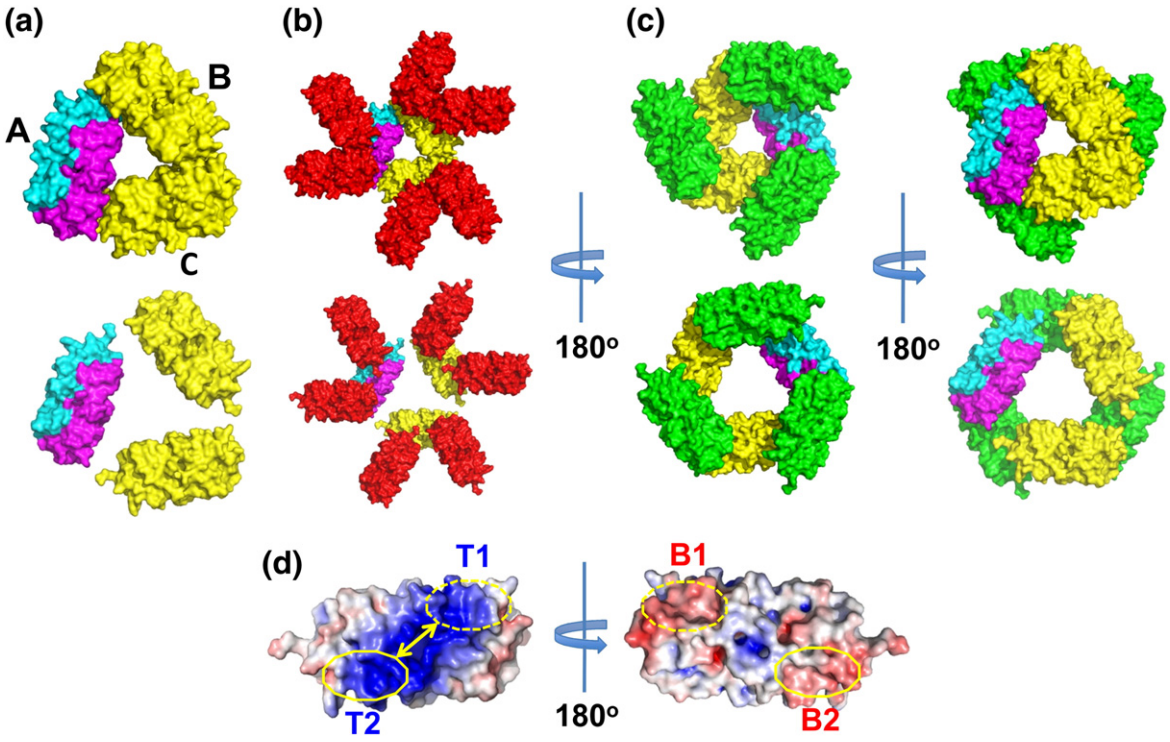

Fig. 2. Inter-dimer interactions observed in XaHspA crystals. (a) XaHspA molecules form two different hexamers (trimer of ACD dimers) in three crystal forms. The hexamer in crystal 3GUF is a closed triangle (top). The hexamers in crystals 3GLA and 3GT6 are open triangles (bottom). Two dimers are colored yellow. The two subunits within the third dimer are colored cyan and magenta, respectively, to show the dimeric building unit. (b) Each hexamer interacts with six dimers (red) from three closed (top in 3GUF) or open (bottom in 3GLA and 3GT6) hexamers above. Two dimers per hexamer (above) are shown. (c) Each hexamer interacts with three dimers (green) from three closed (top in 3GUF) or open (bottom in 3GLA and 3GT6) hexamers underneath. One dimer per hexamer (underneath) is shown. (d) Different electrostatic potentials distributed on the top (left) and bottom (right) surfaces of XaHspA ACD dimer. Circles indicate the interacting sites observed for inter-dimer interactions in crystals. The yellow arrow indicates that binding site T2 can move closer or far away from T1 during dimer–dimer interactions. Electrostatic potentials are colored blue for positive and red for negative. Electrostatic potentials were calculated by APBS wizard in PyMOL (www.umich.edu/~mlerner/Pymol/ and www.umich.edu/~cartsonh/) using default parameters at RT.

sites (T1 to B1 and T2 to B2) from two ACD dimers (Fig. 2b and c), respectively. Because the zone from T1 to T2 has continuous positive electrostatic potentials with a relatively flat surface, the two bound ACD dimers can slide toward each other or away from each other along the positively charged zone (yellow arrow in Fig. 2d) to fit the different distances between two ACD dimers from either a closed or an open XaHspA hexamer. Therefore, the closed and open XaHspA hexamers may be interchangeable, in agreement with the observations that different conditions produced crystals with open hexamers (3GLA and 3GT6) and the same conditions produced both open and closed hexamers in different drops (3GT6 and 3GUF).

The closed XaHspA hexamers in the 3GUF model have direct contacts between adjacent ACD dimers mainly through the C-terminal residues of monomer 1 in ACD dimer A interacting with the C-terminal residues of monomer 2 in ACD dimer B, while the C-terminal residues of monomer 2 in ACD dimer A interacts with the C-terminal residues of monomer 1 in ACD dimer C (top, Fig. 2a). The ACD dimers within the open hexamers have no direct contacts with each other; they are held together by interactions with ACD dimers from different layers in the crystal (Fig. 2c). It is not known if there are interactions between the undefined N-terminal domain and/or the C-terminal extension among these XaHspA dimers like those observed in WHsp16.9 crystal structure.[15] When the ACD dimer of WHsp16.9 structure (PDB code 1GME) was superimposed with any ACD dimer of XaHspA hexamers (closed or open), the N-terminal domain of WHsp16.9 clashed with XaHspA dimers in different layers (Fig. 3). Since the N-terminal domain of WHsp16.9 has the same size (38 amino acid residues) as the undefined N-terminal domain (38–39 amino acid residues) of XaHspA (Fig. 1a), this clash indicates that the N-terminal domain of XaHspA is structurally (in either folding or relative orientation to the ACD dimer or both) different

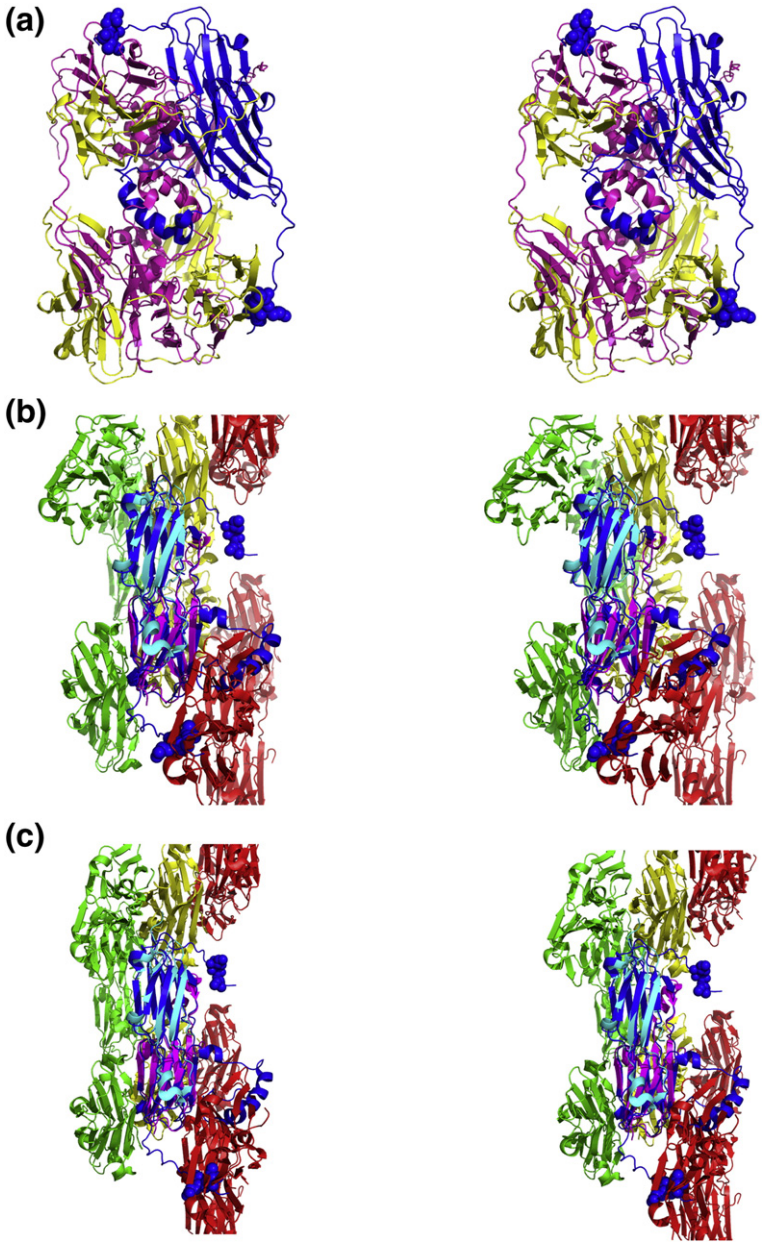

Fig. 3. Structural comparison of WHsp16.9 and XaHspA structures. (a) Stereo view of WHsp16.9 two disks of hexamers. One dimer is colored blue, and the rest of the dimers are colored yellow for one subunit and magenta for the other. Stereo views of XaHspA closed (b) and open (c) hexamers (colored the same as in Fig. 2) and WHsp16.9 dimer (blue). WHsp16.9 ACD dimer was superposed with XaHspA ACD dimer (cyan and magenta) in ribbon diagrams. The IQV motif residues in WHsp16.9 are displayed in spheres.

from the N-terminal domain of WHsp16.9 even though the N-terminal domain of XaHspA is not defined in these XaHspA structures but exists in all crystals. The C-terminal extension of XaHspA contains an IQV sequence (Fig. 1a) similar to the C-terminal "IXI/V" motif in WHsp16.9 and human αB-crystallin, where the IXI/V motif interacts with a neighboring ACD dimer and enhances the oligomerization of these heat shock proteins.[15,18] However, after superposition of the ACD dimer of WHsp16.9 with a XaHspA ACD dimer, the two C-terminal extensions of WHsp16.9 point to two different directions relative to XaHspA ACD dimer: one points to the central hole of the hexamer with no contacts with any neighboring XaHspA ACD dimer, while the other points outward and clashes with an XaHspA ACD dimer from a different layer in the crystal (Fig. 3). Therefore, the IQV motif in the C-terminal extension of XaHspA likely does not interact with the neighboring ACD dimer like its counterpart in WHsp16.9 or human αB-crystallin.

The interaction of XaHspA with LA and insulin

LA and insulin have been used for *in vitro* assays to test the activity of different molecular chaperones. Under reducing conditions such as 10 mM (or above) 1,4-dithiothreitol (DTT)-containing solution, these proteins start to unfold and form irreversible

aggregates. When sHsps are added to this solution, the aggregation is delayed or eliminated.[27–31] In order to investigate the influence of His-tagged residues added to native XaHspA sequence, we compared the chaperone activities of His-tagged XaHspA and non-tagged XaHspA using LA and insulin as substrates for *in vitro* aggregation prevention assay. In these assays, the formation of protein aggregates was monitored by absorbance at 360-nm wavelength. Under reducing conditions (20 mM DTT), reduced LA (LAred) started to aggregate after 50 min of incubation at room temperature (RT) (Fig. 4). When His-tagged XaHspA (Fig. 4a) or XaHspA (Fig. 4b) was added to this solution, LAred aggregation was delayed or eliminated when the amount of His-tagged XaHspA or XaHspA was increased from 10 to 500 μg per 500 μg of LA per reaction. The almost identical profiles for His-tagged XaHspA and XaHspA indicated that no functional differences exist between His-tagged XaHspA and XaHspA as molecular chaperones to prevent LAred from aggregation. Similar results were obtained for His-tagged XaHspA and XaHspA to prevent reduced insulin from aggregation (Fig. 4c and d).

We further analyzed the interactions of His-tagged XaHspA with LA by size-exclusion chromatography

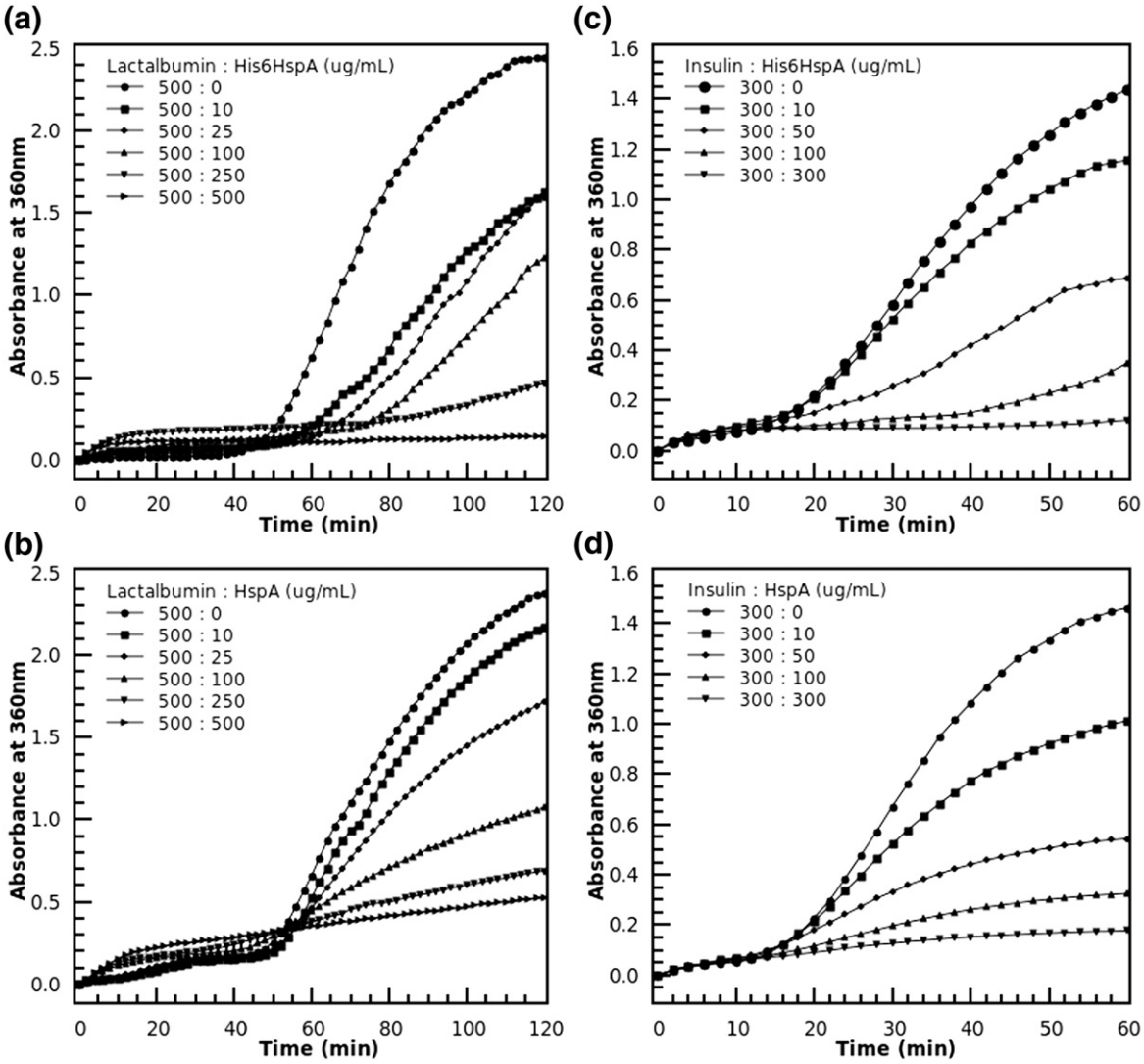

Fig. 4. Dynamic interactions of LAred and reduced insulin with different amounts of His-tagged or non-tagged XaHspA. Profile of apo-LA aggregation (500 μg/mL) induced by DTT in the presence of different amounts of His-tagged XaHspA (His6HspA) (a) or non-tagged XaHspA (HspA) (b). Legend: (●) 0, (■) 10 μg/mL, (♦) 25 μg/mL, (▲) 100 μg/mL, (▼) 250 μg/mL, and (►) 500 μg/mL of His6HspA or HspA in the reaction. Profile of insulin aggregation (300 μg/mL) induced by DTT in the presence of different amounts of His-tagged XaHspA (c) or non-tagged XaHspA (d). Legend: (●) 0, (■) 10 μg/mL, (♦) 50 μg/mL, (▲) 100 μg/mL, and (▼) 300 μg/mL of His6HspA or HspA in the reaction. Protein aggregation was monitored by the increased turbidity at 360 nm at RT in buffered solutions containing 20 mM DTT.

(Fig. 5). In solution, the His-tagged XaHspA protein predominantly exists as an oligomer of molecular mass ~800 kDa, as estimated by size-exclusion chromatography (peak 3 in Fig. 5a and lane 3 in Fig. 5b), indicating an assembly of a 36mer (molecular mass of 756 kDa; one His-tagged XaHspA has a molecular mass of 21 kDa). A very closely related *Xanthomonas* HspA protein, which has the same number (158) of amino acid residues and shares 90% sequence identity with XaHspA, was also observed to form an oligomer of ~800 kDa by size-exclusion chromatography when expressed with a short His-tag at its C-terminus.[32] Similar to the results of the aforementioned *in vitro* chaperone activity assays that the added His-tagged residues did not change the chaperone activity of XaHspA, they did not affect the oligomeric assembly of XaHspA because XaHspA appeared in the peak corresponding to a 36mer with a molecular mass of a little less than 800 kDa. However, XaHspA has significantly less optical absorption than the His-tagged XaHspA protein for the 280-nm UV light used to monitor the protein peaks during chromatography (compare the vertical scales on the left for His-tagged XaHspA and the vertical scales on the right for XaHspA in Fig. 5a). Therefore, we investigated the interactions between His-tagged XaHspA and LA by size-exclusion chromatography. The results should apply to the interactions between XaHspA and LA as it was demonstrated above that the added His-tagged

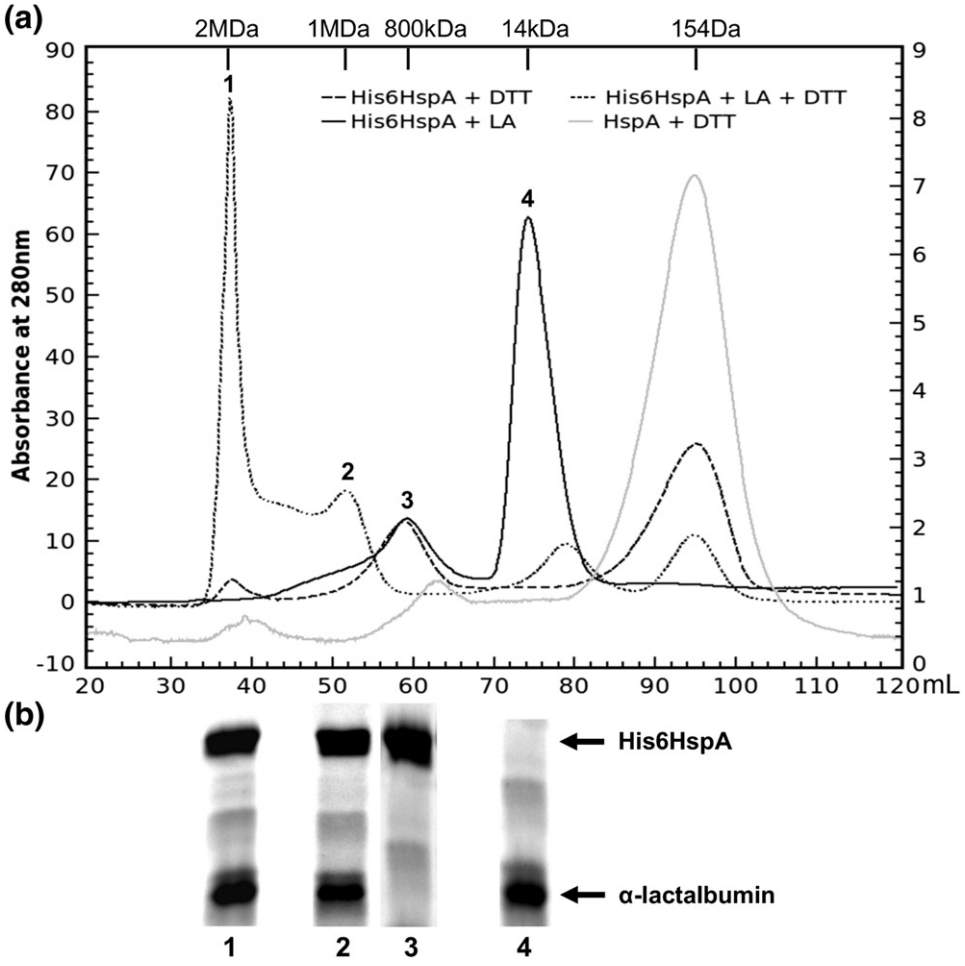

Fig. 5. Oligomerization of XaHspA and interactions with LA. (a) Sephacryl S-400 size-exclusion chromatography of the XaHspA oligomer and complexes associated with LA. His-tagged XaHspA (His6HspA) and apo-LA (3:1, w/w) were mixed and incubated for 60 min with or without 20 mM DTT in 0.5-mL reaction volume to test the protein–protein interaction at RT. Estimated molecular masses are labeled on the top based on standard protein markers. The absorbance at 280 nm on the left side is for profiles involving the His-tagged XaHspA protein, while the absorbance on the right side is for non-tagged XaHspA. (b) SDS-PAGE (15% w/v) analysis of peak fractions collected from S400 size-exclusion chromatography. Lane 1, sample of (HspA–LAred)agg (>2000 kDa, peak 1); lane 2, sample of Xa36m–LAred (~1000 kDa, peak 2); lane 3, sample of Xa36mer (~800 kDa, peak 3); and lane 4, sample of free LA (14 kDa, peak 4).

residues have no noticeable changes in XaHspA in chaperone activity or oligomeric assembly. In the absence of DTT, His-tagged XaHspA appeared at ~800 kDa (36mer), and LA peaked at 14 kDa, showing no association between XaHspA and LA. However, peak 3 has a left shoulder (compare the profile for His6HspA + LA with that of His6HspA + DTT in Fig. 5a), suggesting that a small fraction of LA was denatured even without DTT and interacted with His-tagged XaHspA, leading to polydisperse oligomers of 36mer and larger (both LA and His-tagged XaHspA were detected in the shoulder fractions by SDS-PAGE, Fig. S2b). In the presence of 20 mM DTT, the peak of LAred shifted to the lower-molecular-mass end of the profile (peak 4 in Fig. 5a), suggesting the formation of partially unfolded species. These nonnative LA molecules associated with the 36mers (and other oligomers) of His-tagged XaHspA and caused the His-tagged XaHspA peak (and the left shoulder) to shift to the higher-molecular-mass end (peaks 1 and 2 in Fig. 5a). The 800-kDa oligomer (peak 3 in Fig. 5a) of XaHspA became a 1000-kDa complex (peak 2 in Fig. 5a) of XaHspA–LAred (approximately one LAred per dimer of XaHspA). In addition, very large (molecular mass of >2000 kDa) aggregates, (HspA–LA)agg, were formed (peak 1 in Fig. 5a). It appears that XaHspA–LAred complexes can associate with each other to form polydisperse heterogeneous oligomers (see the shoulder of the XaHspA peak 3 in Fig. 5 and the spectra in the region between peak 2 and peak 1). These heterogeneous oligomers tend to become the larger aggregate with time and increased temperature (Fig. S2a).

Discussion

sHsps are a group of molecular chaperones with diverse sequences and show extremely different organization of oligomeric assemblies even though they share a structurally conserved ACD core for dimerization. Our results suggest one novel mechanism to form polydisperse XaHspA oligomers with the same number of XaHspA monomers but different organizations using either closed or open trimers of XaHspA dimers. Results from size-exclusion chromatography indicated that XaHspA exists predominantly as 36mers in solution. These XaHspA 36mers likely exist in four different conformations as suggested by the inter-dimer interactions in XaHspA crystals (Figs. 2 and6). The basic XaHspA assembly observed in all crystals is either closed or open hexamers (trimers of XaHspA ACD dimers). Therefore, we propose that XaHspA 36mers in solution are formed by stacks of XaHspA hexamers. As mentioned above (Fig. 2), open XaHspA hexamers in crystals are held together by interactions with XaHspA ACD dimers from below or above because there are no direct interactions between ACD dimers within the same open XaHspA hexamer. Therefore, XaHspA 36mers can exist in two different forms: 6mer-6mer-12mer-6mer-6mer (36merA in Fig. 6a, top) or 12mer-6mer-6mer-12mer (36merB in Fig. 6a, bottom). The layer of 12mer is formed by three XaHspA hexamers after each hexamer loses one XaHspA dimer because only two dimers of each XaHspA hexamer can interact with other XaHspA dimers from above and below. The third XaHspA dimer of these open

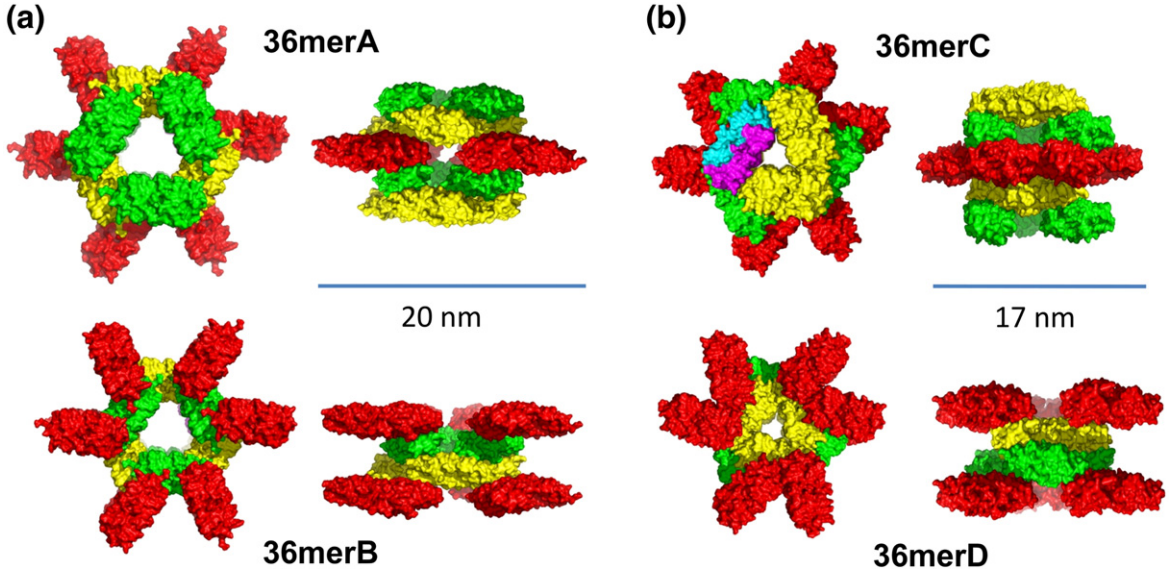

Fig. 6. Four possible conformations of XaHspA 36mers in solution. Based on the inter-dimer interactions observed in crystals (Fig. 2), four different XaHspA 36mers can be constructed. The view from above (left) and side view (right) of XaHspA 36merA (a), 36merB (b), 36merC (c), and 36merD (d). XaHspA 36merA and 36merB (20 nm wide and 8 nm high) are formed by open hexamers. XaHspA 36merC and 36merD (17 nm wide and 8 nm high) is formed by closed hexamers.

hexamers has no interactions with any XaHspA dimers and is therefore not assembled with the 36mers in solution. The inter-dimer interactions between different XaHspA hexamers suggested that the closed and open XaHspA hexamers are interchangeable through the control of the distances between the dimer binding sites T1 and T2; we expect that the closed hexamers have the same stack. Therefore, there are four possible 36mers of XaHspA (36merA–36merAD, Fig. 6). The overall shapes of XaHspA 36mers are very similar with those of 36merC–36merD packed a little more tightly than 36merA–36merB. XaHspA 36merA–36merB (formed by open XaHspA hexamers) is about 20 nm wide and 8 nm high, while 36merC–36merD (formed by closed XaHspA hexamers) is 17 nm wide and 8 nm high (Fig. 6). This possibly reflects different conformations under normal conditions and stress conditions and provides structural evidence in support of the hypothesis that the same sHsp protein exists in different conformations likely with different affinities for substrate binding.[7,11,13,20]

The XaHspA 36mers proposed above have protruding XaHspA dimers (the basic unit for almost all sHsps studied so far) accessible for nonnative protein binding. Similar-shaped oligomers were also reported for human αB-crystallin by studies using solid-state NMR and small-angle X-ray scattering.[19] XaHspA 36mers were observed to directly interact with unfolding LA to form heterogeneous complexes (XaHspA–LA). However, the results of XaHspA–LAred interactions reported here are different from the results reported for some sHsps assays where the aggregation of LA under reducing conditions was delayed or eliminated by sHsps without forming larger aggregates.[27–31] This difference likely reflects the different mechanisms used by XaHspA and other sHsps to protect protein aggregation. It has been proposed that specific hydrophobic regions on some sHsp dimers are potential binding sites to a variety of denatured protein substrates.[33,34] The crystal structures of MjHsp16.5 and WHsp16.9 predicted that these specific hydrophobic regions are blocked by oligomerization.[15,16] Thus, it was suggested that disassembly of sHsps oligomer is a prerequisite for these sHsps to exhibit chaperone-like activity.[21,35,36] However, our results agree with the earlier observation that the activation of yeast sHsp26 does not require dissociation of the oligomer[22] and support the hypothesis that there are at least two states (four possible conformations for XaHspA 36mers) of sHsp oligomers with different affinities for nonnative protein substrates (Fig. 7). The substrate binding sites are not yet identified for XaHspA. If the dimer is the basic functional unit as observed in many sHsps,[21,35,36] there should be two substrate binding sites per dimer because of the 2-fold symmetry observed in the XaHspA dimer (Fig. 7a). Because the top surface of the XaHspA dimer displays electrostatic potentials different from those of the bottom surface, either surface can be used for substrate

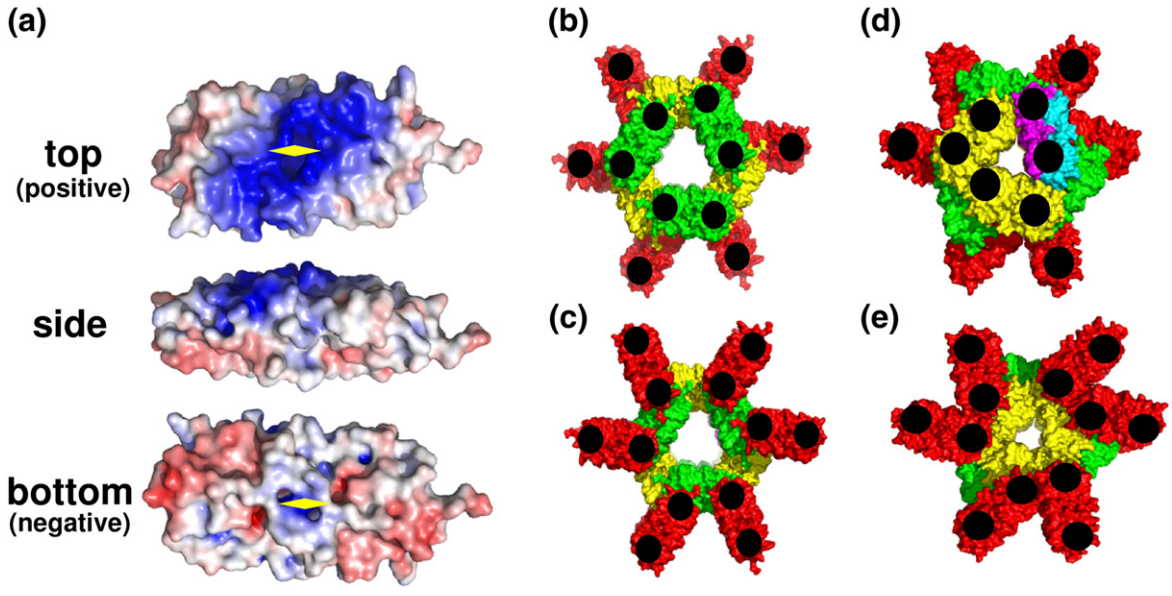

Fig. 7. Nonnative protein binding sites on XaHspA 36merA–36merD. (a) The electrostatic potential surfaces of XaHspA ACD dimer display a 2-fold symmetry. The yellow diamonds indicate the 2-fold symmetry of the ACD dimeric surfaces. Electrostatic potentials are colored blue for positive and red for negative. Electrostatic potentials were calculated by APBS wizard in PyMOL (www.umich.edu/~mlerner/Pymol/ and www.umich.edu/~cartsonh/) using default parameters at RT. (b–e) Substrate binding sites on XaHspA 36merA (b), the top layer of 36merB (c), 36merC (d), and the top layer of 36merD (e). One black circle represents one binding site for a nonnative protein substrate.

binding, but one particular substrate likely binds to one surface only due to the dramatic difference between the two surface electrostatic potentials. Thus, the four XaHspA 36mers will have different substrate binding patterns (Fig. 7b–e). 36merA (open hexamers, 6mer-6mer-12m-6mer-6mer) has six binding sites (black circles) on the first 6mers on the top and six sites on the six protruding dimers in the middle 12mer because another six sites are blocked by the yellow dimers (Fig. 7b). Thus, 36merA has a total of 12 binding sites for nonnative proteins. 36merB (open hexamers, 12mer-6mer-6mer-12mer) has 12 binding sites on the top 12mer (Fig. 7c) but only 6 sites on the bottom 12mer like the middle 12mer of 36merA (red dimers in Fig. 7b), leading to a total of 18 binding sites on 36merB. Similarly, 36merC (closed hexamers, 6mer-6mer-12m-6mer-6mer) has 9 binding sites (6 from the top 6mer and 3 from the middle 12mer) (Fig. 7d), while 36merD (closed hexamers, 12mer-6mer-6mer-12mer) has 15 binding sites (12 on the top 12mer and 3 from the bottom 12mer) (Fig. 7e and d). Therefore, only XaHspA 36merB can interact with LAred to form a complex of one LA per XaHspA dimer, as observed by size-exclusion chromatography (Fig. 5). Together, our results suggest that XaHspA exists in solution as 36mers with four possible conformations, 36merA–36merD. It is not clear which conformation(s) exists or if all of them exist in equilibrium in solution, but the interactions of XaHspA and LAred indicated that XaHspA 36merB, formed by open XaHspA hexamers in 12mer-6mer-6mer-12mer (Fig. 6), is the active oligomer that can form complexes with LAred in a 1:1 dimer:LA ratio.

Experimental Procedures

Protein expression and purification

The HspA gene coding for the protein XaHspA was amplified by PCR from genomic DNA using specific oligonucleotides and subcloned into the expression vector pET-28a (Novagen). His6-tagged HspA protein (His6HspA) was expressed and purified as described previously.[37] In order to produce the non-fusion protein, we amplified the HspA gene from the plasmid construction pET28a-HspA using specific oligonucleotides primers, in which the insertion at the NdeI and BamHI restriction sites of the expression vector pET-3a (Novagen) was allowed. The entire polynucleotide sequence was confirmed. *Escherichia coli* strain BL21(DE3)pLys-S harboring the plasmid construction pET3a-HspA was used to over-express the protein in 3 L of LB broth. Recombinant protein expression was induced overnight at 25 °C and 200 rpm with IPTG to a final concentration of 1 mM. Cells were harvested by centrifugation and resuspended in buffer A (50 mM Tris–HCl, pH 8.0, containing 30 mM NaCl and 1 mM ethylenediaminetetraacetic acid) and disrupted in ice bath by sonication. The total crude extract was clarified by centrifugation at 30,000*g* (20 min, 4 °C). HspA protein from supernatant fraction was precipitated with ammonium sulfate (15% saturation). After centrifugation, protein pellet was suspended in 50 mL of buffer A and dialyzed against the same buffer overnight. Insoluble aggregated material was removed by centrifugation, and the supernatant was loaded onto a 5-mL DEAE-Sepharose Fast Flow column (GE Healthcare). Bound proteins were eluted with a 20-column-volume linear gradient from 0.03 to 1 M NaCl in buffer A. Sample of peak fractions obtained along the ion-exchange chromatography was analyzed by 15% SDS-PAGE. Fractions containing large amount of pure protein were pooled, dialyzed in 50 mM sodium phosphate (pH 6.8) containing 100 mM NaCl (buffer 1), and then concentrated in Amicon Ultracel 30,000 (Millipore). Aliquots were stored at −80 °C for further use.

Size-exclusion chromatography

The sizes of the recombinant His-tagged XaHspA oligomer, non-tagged HspA oligomer, and protein complexes were determined using a Sephacryl S-400 High Resolution column (GE Healthcare), running at 0.2 mL/min in buffer 1. His-tagged XaHspA and apo-LA were prepared in buffer 1. Prior to performing the experiment, we centrifuged the protein samples for 10 min at 12,000*g* to remove insoluble aggregated material and determined the protein concentration. His6HspA (final concentration, 3 mg/mL) and LA (final concentration, 1 mg/mL) were mixed with or without 20 mM DTT. The final sample volumes were 0.5 mL in buffer 1, and the mixture was incubated at RT for 60 min. The entire volume of the final reaction was loaded onto the column without centrifugation. The column was calibrated by Gel Filtration HMW Calibration Kit (GE Healthcare) including blue dextran 2,000,000, thyroglobulin 669,000, ferritin 440,000, aldolase 158,000, and ovalbumin 43,000.

Analysis of protein aggregation by photospectrometry

Recombinant His6HspA, non-tagged HspA, and freshly prepared apo-LA (type III, Sigma) in buffer 2 [50 mM sodium phosphate (pH 6.8) and 100 mM NaCl containing 2 mM ethylenediaminetetraacetic acid] or insulin (bovine pancreas, Sigma) in buffer 3 (50 mM sodium phosphate, pH 7.0, and 100 mM NaCl) were mixed and incubated with different amounts of His6HspA or non-tagged HspA as shown in individual graphs in Fig. 5. Preparation of stock solutions of insulin and apo-LA was performed as described previously.[31] Prior to performing the experiment, we centrifuged each protein sample for 10 min at 12,000*g* at RT and determined the protein concentration. The experiments were performed with or without 20 mM DTT at RT. The final reaction sample volumes were 0.4 mL in buffer 2 or buffer 3. Protein aggregation was monitored immediately after DTT addition by measuring the absorbance at 360 nm in micro cuvettes (0.16 mL, path length of 10 mm) using a GeneQuant 100 (GE Healthcare) spectrophotometer every 2 min for insulin assays and 120 min for apo-LA.

Protein crystallization

Crystals were grown using the sitting-drop vapor diffusion method. Crystallization trials were performed in Chryschem multi-well plates with 300 μL of reservoir solution. Drops consisted of 2 μL of protein solution (7–10 mg/ml in 5 mM Tris–HCl buffer at pH 8.0) and 2 μL of reservoir solution. Crystallization was carried out at 20 °C. Crystals suitable for X-ray data collection were obtained under two different crystallization conditions: (1) 0.1 M Tris–HCl buffer at pH 7.7 containing 1.2 M $(NH_4)_2HPO_4$ (model 3GLA, crystal form I) and (2) 24% (w/v) polyethylene glycol 1500 and 20% glycerol (models 3GT6 and 3GUF, respectively; crystal forms II and III). All crystal forms belong to the *R*3 space group and continue to grow for up to 5 weeks.

Data collection and processing

Crystals were mounted in nylon loops and flash frozen in a nitrogen stream at 100 K in a mother liquor containing 25% glycerol as cryoprotectant. X-ray diffraction intensities were collected at the D03B-MX1 beam-line, Laboratório Nacional de Luz Síncrotron (Campinas-SP, Brazil), using a wavelength of 1.43 Å and an MAR CCD 165 detector (MarResearch). Diffraction data were indexed, integrated, scaled, and merged using the HKL2000 package.[38] Data collection statistics are shown in Table 1.

Structure determination

The structure of the first crystal form was solved by MR using the crystallographic structure of WHsp16.9 (PDB code 1GME),[15] without ions and solvent molecules, as a search model. The rotation and translation searches were performed with the program AMoRe[39] implemented in the CCP4 suite[40] using data from 12 to 3.5 Å. The best solution was obtained using the dimer with the first 45 residues and the last 15 residues removed from both termini and had a correlation coefficient of 36.5% and an R_{crys} of 48.6% after a rigid-body refinement. Refinement was performed using REFMAC 5.2.[41] Cycles of refinement were alternated with rounds of manual model building with Coot[42] using σ_A-weighted $2F_o-F_c$ and F_o-F_c electron density maps. A total of 5% of reflections were used to calculate the R_{free} value throughout the refinement process. The structure of this first crystal form was used to locate XaHspA molecules in the other two crystal forms. Two phosphate groups were further introduced at stereochemically reasonable positions with corresponding strong peaks in the electron density maps in the crystal form I. Some surface residues present partial electron density for the side chains in monomers A and B. Missing residues at both termini could not be traced due to lack of electron density. The final models were analyzed with the program PROCHECK.[43] Refinement and final model statistics are summarized in Table 1.

PDB accession codes

Coordinates and structure factors have been deposited in the PDB with the accession codes 3GT6 (open hexamers) and 3GUF (closed hexamers).

Supplementary materials related to this article can be found online at doi:10.1016/j.jmb.2011.02.004

Acknowledgements

This work was funded by University of California Riverside (to L.F.), The State of São Paulo Research Foundation (grants 01/07536-6 and 03/01646-0 to M.C.B. and The State of São Paulo Research Foundation fellowships to E.H.), and Structural Molecular Biology Network (to F.J.M.M.). E.H. thanks the Laboratório Nacional de Luz Síncrotron for the support during crystal trials and data collection.

References

1. Litt, M., Kramer, P., LaMorticella, D. M., Murphey, W., Lovrien, E. W. & Weleber, R. G. (1998). Autosomal dominant congenital cataract associated with a missense mutation in the human alpha crystallin gene CRYAA. *Hum. Mol. Genet.* **7**, 471–474.
2. Vicart, P., Caron, A., Guicheney, P., Li, Z., Prevost, M. C., Faure, A. *et al.* (1998). A missense mutation in the alphaB-crystallin chaperone gene causes a desmin-related myopathy. *Nat. Genet.* **20**, 92–95.
3. Hsu, A. L., Murphy, C. T. & Kenyon, C. (2003). Regulation of aging and age-related disease by DAF-16 and heat-shock factor. *Science*, **300**, 1142–1145.
4. Clark, J. I. & Muchowski, P. J. (2000). Small heat-shock proteins and their potential role in human disease. *Curr. Opin. Struct. Biol.* **10**, 52–59.
5. Quinlan, R. & Van Den Ijssel, P. (1999). Fatal attraction: when chaperone turns harlot. *Nat. Med.* **5**, 25–26.
6. Sun, Y. & MacRae, T. H. (2005). The small heat shock proteins and their role in human disease. *FEBS J.* **272**, 2613–2627.
7. Haslbeck, M., Franzmann, T., Weinfurtner, D. & Buchner, J. (2005). Some like it hot: the structure and function of small heat-shock proteins. *Nat. Struct. Mol. Biol.* **12**, 842–846.
8. McHaourab, H. S., Godar, J. A. & Stewart, P. L. (2009). Structure and mechanism of protein stability sensors: chaperone activity of small heat shock proteins. *Biochemistry*, **48**, 3828–3837.
9. Narberhaus, F. (2002). Alpha-crystallin-type heat shock proteins: socializing minichaperones in the context of a multichaperone network. *Microbiol. Mol. Biol. Rev.* **66**, 64–93.
10. Van Montfort, R., Slingsby, C. & Vierling, E. (2001). Structure and function of the small heat shock protein/alpha-crystallin family of molecular chaperones. *Adv. Protein Chem.* **59**, 105–156.
11. Sun, Y. & MacRae, T. H. (2005). Small heat shock proteins: molecular structure and chaperone function. *Cell. Mol. Life Sci.* **62**, 2460–2476.
12. Nakamoto, H. & Vigh, L. (2007). The small heat shock proteins and their clients. *Cell. Mol. Life Sci.* **64**, 294–306.

13. Ganea, E. (2001). Chaperone-like activity of alpha-crystallin and other small heat shock proteins. *Curr. Protein Pept. Sci.* **2**, 205–225.
14. Stamler, R., Kappe, G., Boelens, W. & Slingsby, C. (2005). Wrapping the alpha-crystallin domain fold in a chaperone assembly. *J. Mol. Biol.* **353**, 68–79.
15. van Montfort, R. L., Basha, E., Friedrich, K. L., Slingsby, C. & Vierling, E. (2001). Crystal structure and assembly of a eukaryotic small heat shock protein. *Nat. Struct. Biol.* **8**, 1025–1030.
16. Kim, K. K., Kim, R. & Kim, S. H. (1998). Crystal structure of a small heat-shock protein. *Nature*, **394**, 595–599.
17. Bagneris, C., Bateman, O. A., Naylor, C. E., Cronin, N., Boelens, W. C., Keep, N. H. & Slingsby, C. (2009). Crystal structures of alpha-crystallin domain dimers of alphaB-crystallin and Hsp20. *J. Mol. Biol.* **392**, 1242–1252.
18. Laganowsky, A., Benesch, J. L., Landau, M., Ding, L., Sawaya, M. R., Cascio, D. *et al.* (2010). Crystal structures of truncated alphaA and alphaB crystallins reveal structural mechanisms of polydispersity important for eye lens function. *Protein Sci.* **19**, 1031–1043.
19. Jehle, S., Rajagopal, P., Bardiaux, B., Markovic, S., Kühne, R., Stout, J. R. *et al.* (2010). Solid-state NMR and SAXS studies provide a structural basis for the activation of αB-crystallin oligomers. *Nat. Struct. Mol. Biol.* **17**, 1037–1042.
20. Laksanalamai, P. & Robb, F. T. (2004). Small heat shock proteins from extremophiles: a review. *Extremophiles*, **8**, 1–11.
21. Shashidharamurthy, R., Koteiche, H. A., Dong, J. & McHaourab, H. S. (2005). Mechanism of chaperone function in small heat shock proteins: dissociation of the HSP27 oligomer is required for recognition and binding of destabilized T4 lysozyme. *J. Biol. Chem.* **280**, 5281–5289.
22. Franzmann, T. M., Wuhr, M., Richter, K., Walter, S. & Buchner, J. (2005). The activation mechanism of Hsp26 does not require dissociation of the oligomer. *J. Mol. Biol.* **350**, 1083–1093.
23. da Silva, A. C., Ferro, J. A., Reinach, F. C., Farah, C. S., Furlan, L. R., Quaggio, R. B. *et al.* (2002). Comparison of the genomes of two *Xanthomonas* pathogens with differing host specificities. *Nature*, **417**, 459–463.
24. Laia, M. L., Moreira, L. M., Dezajacomo, J., Brigati, J. B., Ferreira, C. B., Ferro, M. I. *et al.* (2009). New genes of *Xanthomonas citri* subsp. *citri* involved in pathogenesis and adaptation revealed by a transposon-based mutant library. *BMC Microbiol.* **9**, 12.
25. Larkin, M. A., Blackshields, G., Brown, N. P., Chenna, R., McGettigan, P. A., McWilliam, H. *et al.* (2007). Clustal W and Clustal X version 2.0. *Bioinformatics*, **23**, 2947–2948.
26. DeLano, W. L. (2002). *The PyMOL Molecular Graphics System.* DeLano Scientific, San Carlos, CA..
27. Bettelheim, F. A. (2002). Kinetics of chaperoning of dithiothreitol-denatured alpha-lactalbumin by alpha-crystallin. *Int. J. Biol. Macromol.* **30**, 161–169.
28. Bova, M. P., Yaron, O., Huang, Q., Ding, L., Haley, D. A., Stewart, P. L. & Horwitz, J. (1999). Mutation R120G in alphaB-crystallin, which is linked to a desmin-related myopathy, results in an irregular structure and defective chaperone-like function. *Proc. Natl Acad. Sci. USA.* **96**, 6137–6142.
29. Lindner, R. A., Kapur, A. & Carver, J. A. (1997). The interaction of the molecular chaperone, alpha-crystallin, with molten globule states of bovine alpha-lactalbumin. *J. Biol. Chem.* **272**, 27722–27729.
30. Ecroyd, H. & Carver, J. A. (2008). The effect of small molecules in modulating the chaperone activity of alphaB-crystallin against ordered and disordered protein aggregation. *FEBS J.* **275**, 935–947.
31. Horwitz, J., Huang, Q. L., Ding, L. & Bova, M. P. (1998). Lens alpha-crystallin: chaperone-like properties. *Methods Enzymol.* **290**, 365–383.
32. Lin, C. H., Lee, C. N., Lin, J. W., Tsai, W. J., Wang, S. W., Weng, S. F. & Tseng, Y. H. (2010). Characterization of *Xanthomonas campestris* pv. *campestris* heat shock protein A (HspA), which possesses an intrinsic ability to reactivate inactivated proteins. *Appl. Microbiol. Biotechnol.* **88**, 699–709.
33. Jiao, W., Qian, M., Li, P., Zhao, L. & Chang, Z. (2005). The essential role of the flexible termini in the temperature-responsiveness of the oligomeric state and chaperone-like activity for the polydisperse small heat shock protein IbpB from *Escherichia coli*. *J. Mol. Biol.* **347**, 871–884.
34. Basha, E., Friedrich, K. L. & Vierling, E. (2006). The N-terminal arm of small heat shock proteins is important for both chaperone activity and substrate specificity. *J. Biol. Chem.* **281**, 39943–39952.
35. Haslbeck, M., Walke, S., Stromer, T., Ehrnsperger, M., White, H. E., Chen, S. *et al.* (1999). Hsp26: a temperature-regulated chaperone. *EMBO J.* **18**, 6744–6751.
36. Giese, K. C. & Vierling, E. (2002). Changes in oligomerization are essential for the chaperone activity of a small heat shock protein *in vivo* and *in vitro*. *J. Biol. Chem.* **277**, 46310–46318.
37. Hilario, E., Teixeira, E. C., Pedroso, G. A., Bertolini, M. C. & Medrano, F. J. (2006). Crystallization and preliminary X-ray diffraction analysis of XAC1151, a small heat-shock protein from *Xanthomonas axonopodis* pv. *citri* belonging to the alpha-crystallin family. *Acta Crystallogr., Sect. F: Struct. Biol. Cryst. Commun.* **62**, 446–448.
38. Otwinowski, Z. & Minor, W. (1997). Processing of X-ray diffraction data collected in oscillation mode. *Methods Enzymol.* **276**, 307–326.
39. Navaza, J. (1994). AMoRe: an automated package for molecular replacement. *Acta Crystallogr., Sect. A: Found. Crystallogr.* **50**, 157–163.
40. Collaborative Computational Project, Number 4. (1994). The CCP4 suite: programs for protein crystallography. *Acta Crystallogr., Sect. D: Biol. Crystallogr.* **50**, 760–763.
41. Murshudov, G. N., Vagin, A. A., Lebedev, A., Wilson, K. S. & Dodson, E. J. (1999). Efficient anisotropic refinement of macromolecular structures using FFT. *Acta Crystallogr., Sect. D: Biol. Crystallogr.* **55**, 247–255.
42. Emsley, P., Lohkamp, B., Scott, W. G. & Cowtan, K. (2010). Features and development of Coot. *Acta Crystallogr., Sect. D: Biol. Crystallogr.* **66**, 486–501.
43. Laskowski, R. A., MacArthur, M. W., Moss, D. S. & Thornton, J. M. (1993). PROCHECK: a program to check the stereochemical quality of protein structures. *J. Appl. Crystallogr.* **26**, 283–291.